ELSEVIER

Journal of Alloys and Compounds 317–318 (2001) 52–59

Journal of ALLOYS AND COMPOUNDS

www.elsevier.com/locate/jallcom

Crystallochemistry and Kondo-like behaviour of the thorium and uranium arsenoselenides

Z. Henkie*, A. Pietraszko, A. Wojakowski, L. Kępiński, T. Cichorek

W. Trzebiatowski Institute for Low Temperature and Structure Research, Polish Academy of Sciences, P.O. Box 1410, 50-950 Wrocław 2, Poland

Abstract

We have grown single crystals of uranium and thorium arsenoselenide and arsenosulphide by the chemical vapour transport method. The crystals show a Kondo-like effect and its contribution to the resistivity was estimated by the determination of the reciprocal residual resistivity ratio (RRRR) $\rho(4,2)/\rho(300)$. The ratio varied from 0.70 (for UAsS) to 2.10 (for ThAsSe). A high resolution transmission electron microscopy study of ThAsSe crystals reveals a perfect ordering of cations. The X-ray diffraction examination showed that the unit cells of the examined crystals belong to a tetragonal system with the PbFCl-type structure (space group *P4/nmm* (no. 129)). Anomalously large anisotropic displacement factors have been observed for all the atoms composing the compounds examined. An interdependence between the displacement factor and RRRR has allowed to ascribe both phenomena to the same source. It indicates that the two-level system Kondo model is most suitable for the theoretical description of the systems. © 2001 Elsevier Science B.V. All rights reserved.

Keywords: Intermetallics; Kondo effects; Crystal structure and symmetry

1. Introduction

Our motivation for this study comes from the earlier observation that the electrical resistivity of the uranium arsenoselenide can be univocally resolved into three temperature dependent contributions: namely the spin-disorder resistivity $\rho_S(T)$, phonon resistivity $\rho_{ph}(T)$ and single-ion Kondo-like resistivity $\rho_K(T)$ [1,2]. This compound becomes ferromagnetic below about 110 K [3–5] but the single-ion Kondo-like resistivity persists also in the ferromagnetic state [2]. Usually, the ferromagnetism should block out any possibility of spin flip of the magnetic ion at the scattering of conduction electrons and thus the magnetic Kondo effect is not expected [6]. Besides that, the examination of thermoelectric power and Hall resistivity of the uranium arsenoselenide [7] has shown some anomalous behaviour, which could be explained by assuming that the Kondo scattering does contribute to these physical quantities. On the other hand, an examination of the magnetoresistivity of UAsSe at helium temperature [7,8] has indicated that this Kondo scattering is of a nonmagnetic origin.

Several types of nonmagnetic Kondo models have recently been intensively examined. For example, two types of models have been considered in order to explain the Kondo-like behaviour in the uranium arsenoselenide [7,8]. They are: (1) quadrupolar Kondo model for the U^{4+} ion in cubic symmetry [9], and (2) two-level system (TLS) Kondo model [10–13]. An idea of the possible relevance of the TLS Kondo model to the case of UAsSe is based upon a partial anion disorder observed in neutron diffraction studies [8].

The uranium arsenoselenide crystallises in the tetragonal PbFCl-type (*P4/nmm*) structure which can be described as consisting of stacked layers along the *c*-axis with the sequence: As–U–Se–Se–U–As [14,15]. Neutron diffraction experiment performed on a UAsSe single crystal, with Curie temperature T_C equal to 108 K, showed that about 6% of As-atom positions are occupied by the Se-atoms and vice versa [8]. The studies of the temperature dependence of the *ab*-plane [16,17] resistivity of the uranium arsenochalcogenides — UAsS, UAsSe and UAsTe have pointed out some unique positions of the uranium arsenoselenide among these three compounds. It turns out that an observed extended upturn in the resistivity of UAsSe below about $0.5T_C$ is characteristic only for this compound.

This exceptionally extended Kondo-like resistivity behaviour and their nonmagnetic features, observed for this compound, may originate from the anion disorder. Because

*Corresponding author.

0925-8388/01/$ – see front matter © 2001 Elsevier Science B.V. All rights reserved.
PII: S0925-8388(00)01356-6

of a small difference between the covalent radii of arsenic (1.20) and selenium (1.16) a formation of the anion disorder is presumably easier in UAsSe than in the other two uranium arsenochalcogenides. If the observed Kondo effect is really of a nonmagnetic origin and is due to the TLS formation which originates from the anion disorder then one should expect that the nonmagnetic Kondo scattering effect is also present in ThAsSe. Thus, the aim of this paper is to show that our outlook is the correct one. The crystallochemical examination of the thorium and uranium arsenoselenides and arsenosulphides should give an indication on the origin of the nonmagnetic Kondo effect in this group of compounds.

2. Experimental

We have grown uranium and thorium arsenosulphide and arsenoselenide crystals by the chemical vapour transport (CVT) method. In the case of uranium-based compounds, the metallic U with As and S or Se, were mixed together in desired molar ratios, and then this mixture was sealed in the evacuated silica tube with bromine as transporting agent. About 3–5 mg of Br_2 per cubic centimetre of the ampoule volume was used. At the first step, during a gradual increase of temperature, from 400 to 950°C, the elements reacted giving a powder product. Then, the substrate was homogenised for a few days. Finally, the ampoule was placed at the temperature gradient of 950→900°C for a few weeks and the plate-like crystals (of *ab* face up to 25 mm^2 and 1 mm thick along the *c*-axis) grew at the lower temperature end of the tube. We have grown single crystals from substrates of different compositions and at different temperature of the lower temperature zone ranging from 920 to 880°C.

It was found that the RRRR of obtained UAsS crystals was equal to 0.7 and their ferromagnetic transition temperature was close to 117 K. Both these quantities are hardly dependent on changes of the growing condition. To get a different As/Se atomic content ratio (ACR) and hence a different amount of anion disorder in a given crystal, we have applied different conditions of growing single crystals of the uranium arsenoselenide. As a result, the values of the RRRR ranged from 1.54 to 0.92 and the Curie temperatures from 102 to 116 K.

The crystals having the lowest T_C values were found either between crystals grown from substrates of stoichiometric composition or from substrates having an ACR$<$1. This is presumably due to a temperature gradient along the lower temperature zone, where the crystals with a slightly different T_C grew at different places on the tube. By lowering the As/Se ACR of the substrate the contribution of the lower T_C crystals was increased. However, a decrease in the As/Se ACR down to 0.6, has not resulted in growing crystals with $T_C<101.5$ K. On the other hand, the crystals with the highest T_C ($T_C=116$–118 K) were obtained from the substrate of composition given by the formula: $U_{1.05}AsSe$.

The natural surfaces of seven uranium arsenoselenide crystals, having T_C between 102 and 113 K, were investigated by scanning electron microscopy with energy dispersive X-ray (EDAX) microanalysis. Using the standardless analysis procedure and assuming that a selected crystal with $T_C=113$ K has stoichiometric composition [18], we have established that the composition of the crystal with $T_C=102$ K should be described by the index $x=0.05$ in the chemical formula $UAs_{1-x}Se_{1+x}$. This composition turns out to be quite different from the substrate composition described by $x=0.25$. The composition of the remaining crystals expressed by the As/Se ACR equal to $r=(1-x)/(1+x)$ could be roughly approximated by the equation:

$$r = 0.021 + 8.7\times10^{-3}T_C. \quad (1)$$

To grow the ThAsSe and ThAsS single crystals, the inner wall of the silica tube was covered with a layer of pyrolytic carbon in order to protect it from possible reaction of thorium with the silica. It was necessary to modify some procedures applied in the case of uranium compounds. Firstly, the elemental Th, As and Se or S, in amounts corresponding to a composition of $0.9ThAsSe(S)+0.1ThAs_2$, were placed in an alumina crucible, sealed in an evacuated silica tube and slowly heated until the powder mixture was obtained. Then the mixture was transported into the silica tube with walls covered by the pyrolytic carbon and sealed again together with bromine as in the case of uranium compounds. The chemical transport from the 1020°C zone to that of the 970°C one, lasted for 10 or 14 days. As a result, single crystals of ThAsSe having, in the limit of accuracy of the EDAX microanalysis, a stoichiometric composition together with the crystals of the $ThAs_{1.5}S_{0.5}$ composition were obtained. The chemical formulae for the thorium compounds were determined by the standard EDAX microanalysis of the natural crystal surfaces.

Single crystals of all thorium and uranium arsenosulphides and arsenoselenides were examined by X-ray diffraction, and also by the determination of both their Curie temperatures and RRRRs. An electron microscopy examination has only been done for the ThAsSe. The examined uranium arsenoselenide crystals come from three different crystal growing runs, which are labelled with numbers 101, 108 and 116. The numbers refer to values of the Curie temperature of the most typical crystals for the particular growing run. The label is sometimes completed with a number of the examined crystal from the particular run.

The high resolution transmission electron microscopy (HRTEM) and selected area electron diffraction (SAED) studies of ThAsSe crystals were performed with Philips CM20 SuperTwin microscope operated at 200 kV and providing resolution of 0.24 nm.

Single crystal X-ray diffraction (XRD) intensity data were collected at room temperature of 296 K using a four circle X-ray diffractometer KM4-CCD (KUMA DIFFRACTION Company) with Mo Kα radiation (λ= 0.71073 Å).

3. Kondo-like behaviour of the thorium and uranium arsenoselenides

In the case of a ferromagnetic metal, showing a nonmagnetic Kondo effect, we may expect that the electrons are scattered by: the dynamic centres, the spin disorder of the ferromagnetic matrix, the phonons, and the static impurities. All these different scattering mechanisms contribute to the total resistivity $\rho(T)$, with the following components $\rho_K(T)$, $\rho_S(T)$, $\rho_{ph}(T)$, and ρ_0, respectively. In our model, we assume that the $\rho_S(T)$ contribution is the only one that responds to the ferromagnetic phase transition. Thus it is the only one resistivity contribution that is responsible for a strong change of a slope of the $\rho(T)$ dependence at T_C. Though, Oppeneer [19] was able to interpret the Kerr effect data of UAsSe [20,21] in terms of the itinerant model for the 5f electrons, there is much stronger evidence of the 5f electrons' localization. For example, the magnetoresistivity measured near T_C [22], photoemission experiments [23,24] or diffraction of polarised neutrons on the ferromagnetic UAsSe (T_C=108 K) [15] have shown that the uranium $5f^2$ electrons are localised. Thus, it is very probable that the spin disorder in the arsenoselenide is controlled by the RKKY interactions, which are assumed to be isotropic. The Matthiessen rule allows one to write the resistivity tensors along the *c*- and *a*-axes for the tetragonal system as follows:

$$\rho^c(T) = \rho_0^c + \rho_{ph}^c(T) + \rho_S^c(T) + \rho_K^c(T) \quad (2)$$

$$\rho^a(T) = \rho_0^a + \rho_{ph}^a(T) + \rho_S^a(T) + \rho_K^a(T). \quad (3)$$

The subtraction of Eq. (3) from Eq. (2) gives $\Delta\rho(T)$ being only a linear combination of Kondo, phonon and residual contribution, if the spin disorder contribution is assumed to be isotropic:

$$\Delta\rho(T) = \rho_0^c - \rho_0^a + [\rho_{ph}^c(T) - \rho_{ph}^a(T)] + [\rho_K^c(T) - \rho_K^a(T)]. \quad (4)$$

Thus, such a behaviour was observed for the uranium arsenoselenide single crystal having T_C=102 K [2]. The temperature dependencies of the resistivity tensors $\rho^c(T)$ and $\rho^a(T)$ just for this crystal are shown in the inset of Fig. 1. The resistivity versus temperature dependence for each tensor shows an anomaly at T_C due to the appearance of long range magnetic order below T_C. The anomaly is due to a strong change of a slope of the $\rho_S(T)$ contribution at T_C [25]. The absence of an anomaly in the $\Delta\rho(T)$ curve

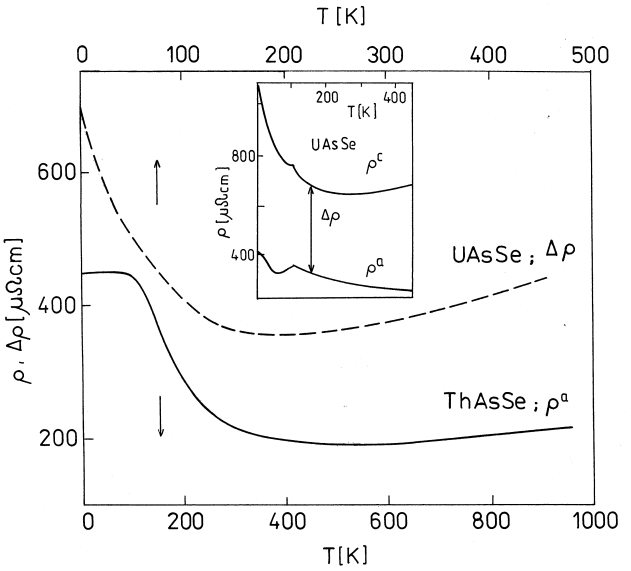

Fig. 1. Temperature dependence of the resistivity along the *a*-axis for ThAsSe (from Ref. [17]) and the result of subtraction of the *a*-axis resistivity from the *c*-axis resistivity $-\Delta\rho(T)$ in the case of UAsSe (from Ref. [2]). Inset: the total resistivity tensors along the *c*-axis — $\rho^c(T)$ — and along the *a*-axis — $\rho^a(T)$ — for UAsSe sample having T_C=102 K.

proves the absence of the spin disorder component. Moreover, it was shown in Ref. [2] that between 40 and 440 K, $\Delta\rho(T)$ for the uranium arsenoselenide was approximated by the formula:

$$\Delta\rho(T) = \text{constant} + C_{ph}T - C_K \log T. \quad (5)$$

This formula corresponds well to the original Kondo formula given in 1964 [26].

The ThAsSe crystals are composed of nonmagnetic atoms and hence the spin-disorder resistivity component is absent in their total resistivity. This can be directly compared to the $\Delta\rho(T)$ curve of UAsSe, characterised by T_C=102 K, and to such data of Schoenes et al. [17] for the *a*-axis resistivity of ThAsSe which is schematically shown by the solid line in Fig. 1. Note that the temperature scale for UAsSe is enlarged by a factor of 2. Both the $\Delta\rho(T)$ curve for UAsSe and the $\rho^a(T)$ curve for ThAsSe are similar to each other above 100 K and have the shape characteristic for a single-ion Kondo system. This additionally proves the nonmagnetic origin of the Kondo type behaviour of the resistivity of these compounds.

4. Examination of ThAsSe with electron transmission microscopy

Samples for HRTEM study were prepared by dipping a copper microscope grid (covered with holey carbon) into the fine powder obtained by grinding crystallites of

ThAsSe in a mortar and pestle. This procedure allowed to observe many small crystals oriented in various ways according to the electron beam. Well developed diffraction patterns with sharp spots were observed. No indications of a superstructure or the cation disorder were found for all the ThAsSe crystals studied. Similarly, high resolution images of the crystals revealed extensive regions (at least up to 1000 Å) of undisturbed lattice fringes and showed no defects originating from crystal growing.

As an example, Fig. 2 shows a high resolution image of ThAsSe crystal wedge in its [100] axis orientation (ED pattern is included as the inset of this figure). From the image it is seen that the crystal exhibits a well ordered structure over long distances (at least 400 Å) without indication of microtwins or ordered defects. (An amorphous layer seen at the edge of the crystal comes from its surface oxidation and from a carbon contamination — hydrocarbon residue in the electron microscope). Some contrast changes observed in the direction perpendicular to the crystal edge are due to a change of the thickness of particular crystals. We have applied the CIP (crystallographic image processing) procedure performed with CRISP package [27] to the portion of the image presented in Fig. 2. In Fig. 3 a magnified portion of the image (the thinnest part of a crystal close to the edge shown in Fig. 2) is presented after digitalisation. An inset in Fig. 3 shows the same image after application of the CIP procedure. Analysis of the Fourier transform of an amorphous area of the image revealed that the image was recorded at the Scherzer defocus with practically no astigmatism. Thus the thinnest area of the crystal should be directly interpretable as the projection of the crystal potential. It has been established that the symmetry of the image is best assigned to two dimensional *Pmg* space group with a rectangular cell having dimensions of 4.1 and 8.6 Å.

This result agrees well with the crystal data determined for ThAsSe by the XRD method clearly demonstrated in Fig. 3, where a model of the structure is shown, too. Furthermore, it is seen that the thorium ions are imaged as black dots and positioned at the proper sites. However, due to the limited resolution of our microscope, the positions of As and Se ions within the unit cell could not be seen clearly. Also, due to closeness in the atomic numbers of As and Se their eventual exchange in the unit cell would not have any effect on the image.

Fig. 4 shows HRTEM image of the same crystallite oriented along the [1$\bar{1}$0] direction, i.e. parallel to that of the

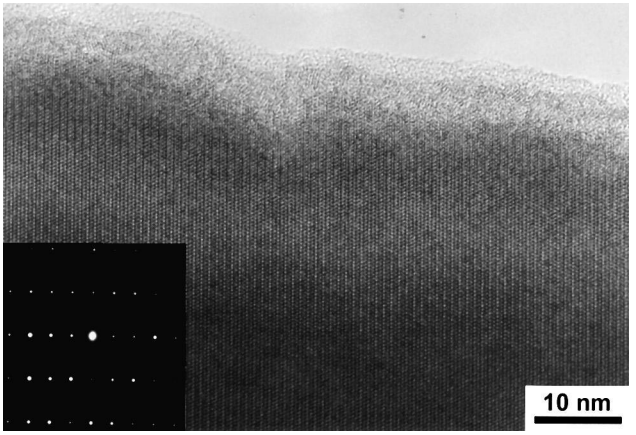

Fig. 2. HRTEM image and corresponding SAED pattern (inset) of the ThAsSe crystal in [100] orientation.

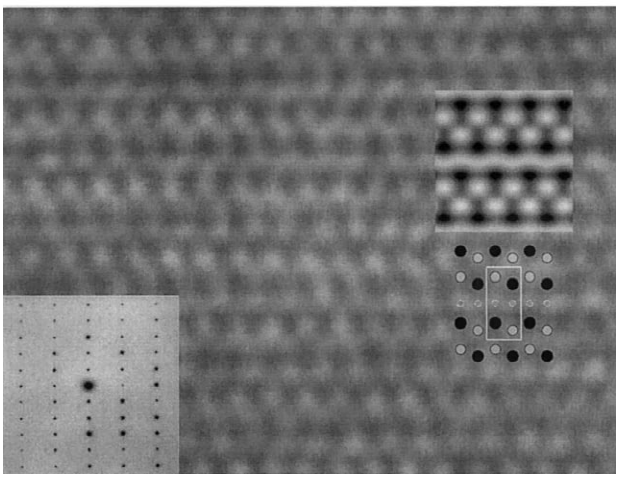

Fig. 3. Magnified portion of the image from Fig. 2. As the insets are shown, the SAED pattern, CIP processed image and the model of the crystal structure.

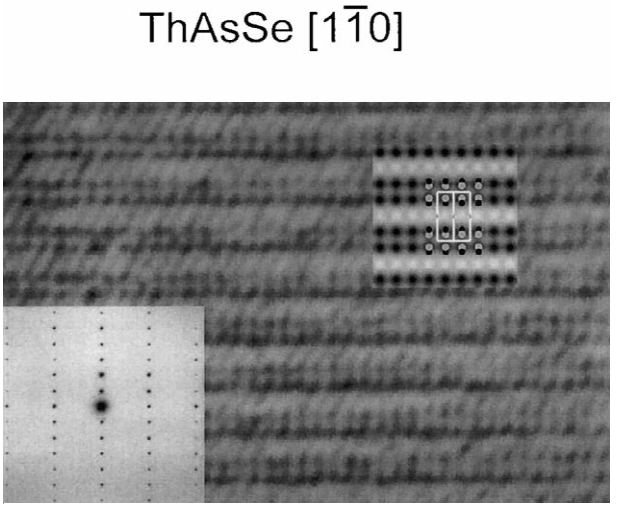

Fig. 4. HRTEM image of the ThAsSe crystal in [1$\bar{1}$0] orientation. As the insets are shown, the SAED pattern, CIP processed image and the model of the crystal structure.

electron beam. Again, good correspondence between the image and the model of the structure is observed.

5. X-ray diffraction examination

The crystal structure of UAsSe was determined using the X-ray method for the following samples: two samples of UAsSe-116 (sphere $r=0.23$ mm), three samples of UAsSe-108 (sphere $r=0.12$; 0.15; 0.17 mm) and two samples of UAsSe-101 (irregular shape). The crystal structure determination for UAsS, ThAsS and ThAsSe have been performed from two selected samples for each compound. X-ray intensity data were collected using a two dimensional CCD detector in eight runs on 120° omega angle using step 0.74° and 25 s exposures for each frame. For each crystal as many as 3200 reflections were recorded to a resolution of about 0.55–0.65 which merged to give about 160–240 non-equivalent reflections.

The lattice parameters were calculated for each sample from all the collected reflections with intensity $I(hkl) > 10\sigma$. The accuracy of the lattice parameters was within $\Delta a/a = 5 \times 10^{-4}$. The XRD examination showed that the unit cells of all the examined crystals belong to a tetragonal system of the PbFCl-type structure. The crystal structures were refined using SHEL97 programs system for the *P4/nmm* (no. 129) space group, where the atoms occupy the following Wyckoff positions:

U(Th)	2*c*	(4 mm)	0.25	0.25	*z*
As	2*b*	(−4m2)	0.25	0.75	0.50
Se(S)	2*c*	(4 mm)	0.25	0.25	*z*

The XRD examinations have determined the composition for thorium arsenosulphide as $ThAs_{1.23}S_{0.77}$ and the stoichiometric composition 1:1:1 for the remaining compounds. However, this result needs additional comment. When the refinement of the crystal structure of UAsS and UAsSe is made on the assumption that the As/Y ACR (Y=S or Se) is constant and equal to 1, and automatic adjustment of varying occupation of the As position by Y anion and vice versa starts from the disordered state, then the refinement ends with completely ordered structure in the case of UAsS. However, in the case of UAsSe the refinement ends with the structure having about 17% of selenium positions occupied by As and vice versa, while the reliability factor for this structure is the same as in the case when the refinement for the ordered structure is done. The neutron diffraction experiment performed for the same crystal ($T_C=108$ K) [15] gives merely 6% of the disorder in the occupation of the anion sites. It means that the XRD is not a sufficient method for the determination of the As/Se ACR in the uranium and thorium arsenoselenides.

The possible change of the As/Se ACR in the uranium arsenoselenide samples examined here is of the order of 12%. This value was estimated from Eq. (1). Any detection of such a small change in the As/Se ACR seems to be beyond the sensitivity of the XRD method in the case of atoms, the electron sphere of which differs from one to another by one electron only. In the case of the thorium arsenosulphide, the composition determined by EDAX differs from that determined by XRD. However, both the values are consistent in this sense that the As/S ACR $\gg 1$. The temperature dependence of the resistivity for the thorium arsenosulphide differs from that of either thorium or uranium arsenoselenides. Though, the residual resistivity for the thorium arsenosulphide is large, nevertheless, it depends weakly on temperature with no clear indication of the single ion Kondo-like scattering [28]. Therefore we exclude this compound from further consideration.

Finally it is worth mentioning that the XRD refinement of the crystal structure of the UAsSe-116 samples reveals the presence of about 3.5% of uranium atoms being shifted from the uranium lattice positions. They however keep their point symmetry, being the same as that of the other uranium atoms. The projection of the crystal structure with some additional positions of U atoms is presented in Fig. 5. These additional positions are shifted from those of the U_1 one by an average distance of ~0.7 Å and 0.5 Å in the UAsSe-116-1 and UAsSe-116-2 samples, respectively. The occupation factor for the U_2 and U_3 positions is equal to 2% and 1.5%, respectively. The origin of this behaviour and its physical consequences requires further studies.

The crystal structure parameters determined for the investigated crystals are collected in Table 1. Table 2 in turn, collects the data which are essential for the topics of this paper. They are: (i) the anisotropic displacement factor of all ions composing ThAsSe, UAsSe and UAsS, and (ii) the difference between the unit cell volume for ThAsSe and that of UAsSe (ΔV). Any existing relation of these quantities to the RRRR seems to be the most interesting matter of our study.

The meaning of the above mentioned quantities is the following. The high value of the anisotropic displacement factor reveals an instability in the occupation of the lattice

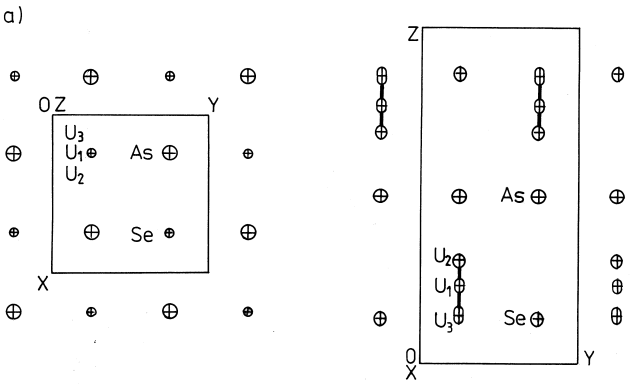

Fig. 5. Projection of the crystal structure with additional positions of U atoms (U_2,U_3) for the UAsSe-116 samples along the *c*-axis (a) and the *a*-axis (b).

Table 1
Comparison of the crystal data for the samples with different T_C

Formula-label	a (Å) $\pm\sigma=0.001$	c (Å) $\pm\sigma=0.001$	V (Å^3) $\pm\sigma=0.002$	Density (Mg/m^3)	d (Å)=U1–S, U1–Se, Th1–S, Th1–Se	d (Å)=U1–As, Th1–As	$X_{U\ or\ Th}$ (coordinates $\times10^{-4}$)	$X_{Se\ or\ S}$ (coordinates $\times10^{-4}$)	R and R_w factor (%)	N-unique reflections
ThAsSe	4.0840	8.578	143.04	8.960	3.0119	3.0829	2308	1309	5.97, 14.74	105
$ThAs_{1.23}S_{0.77}$	4.0225	8.483	137.26	8.441	2.9419	3.1068	2209	1323	5.14, 13.53	179
UAsSe-101	4.000	8.400	134.40	9.684	2.9474	3.0126	2304	1317	4.44, 8.77	284
UAsSe-108-1	3.995	8.396	134.00	9.713	2.9442	3.0198	2303	1314	5.46, 13.17	335
UAsSe-108-2	3.998	8.402	134.30	9.692	2.9464	3.0212	2304	1316	5.09, 10.96	359
UAsSe-108-3	3.997	8.408	134.39	9.685	2.9464	3.0238	2302	1315	3.15, 7.79	259
UAsSe-116-1	3.976	8.381	132.53	9.821	2.9292	3.0135	2298	1319	4.31, 10.63	304
UAsSe-116-2	3.977	8.367	132.44	9.828	2.9307	3.0110	2299	1318	5.48, 13.20	254
UAsS	3.860	8.128	121.10	9.461	2.8084	3.0154	2150	1336	2.22, 4.41	260

Table 2

Formula-label	T_C (K)	RRRR[a]	Anisotropic thermal displacement factors $\langle u_2\rangle$ (Å^2)$\times10^4$						ΔV[b] (A^3)
			U(Th) u_{11}	U(Th) u_{33}	As u_{11}	As u_{33}	Se(S) u_{11}	Se(S) u_{33}	
ThAsSe	Paramagn.	2.10	223	371	302	326	176	316	–
$ThAs_{1.23}S_{0.77}$	Paramagn.	0.90	152	67	197	92	121	89	–
UAsSe-101	102	1.54	170	130	222	92	145	120	8.64
UAsSe-108-1	110.2	1.18	85	97	127	85	76	85	9.04
UAsSe-108-2	107.7	1.25	66	118	121	92	62	99	8.78
UAsSe-108-3	110.5	1.17	102	98	147	73	91	95	8.65
UAsSe-116-1	115.1	0.95	50	101	93	73	51	87	10.51
UAsSe-116-2	116.5	0.92	42	71	86	61	34	90	10.60
UAsS	117	0.70	50	62	73	42	63	44	–

[a] RRRR = $\rho(4.2)/\rho(300)$.
[b] $\Delta V = V_{ThAsSe} - V_{UAsSe}$.

positions and may be considered as the property related to the TLS formation. This may also mean that some atoms hop between two positions separated by a small distance, thus forming the TLS scattering centre. One can see in Table 2 that the displacement factor for all the ions of the compounds varies with the RRRR, however, to make our discussion easier we will focus on the most extending one — the As u_{11}. One of the simplest measures of the hybridisation between the 4f or 5f electrons with electrons of the respective conduction bands is the unit cell volume contraction ΔV of a given f-electron compound with respect to its homologous compound without the f-electrons [29]. The interpretation that the increase in ΔV is due to the hybridisation only may be supported by an observation that this increase is accompanied by the increase in the electron specific heat coefficient γ of the UAsSe crystals by a factor of about 2 [30,31], when one is passing from the crystals having $T_C \approx 110$ K to the crystals exhibiting $T_C \approx 116$ K. Finally the RRRR is a measure of the Kondo-like resistivity at helium temperature in terms of the room temperature resistivity of a given sample.

Both the ΔV and As u_{11} quantities are plotted versus the RRRR in Fig. 6. The solid (ΔV) and broken (As u_{11}) lines are guides for the eye. There is no simple relation between ΔV and RRRR, because of the fact that they may originate

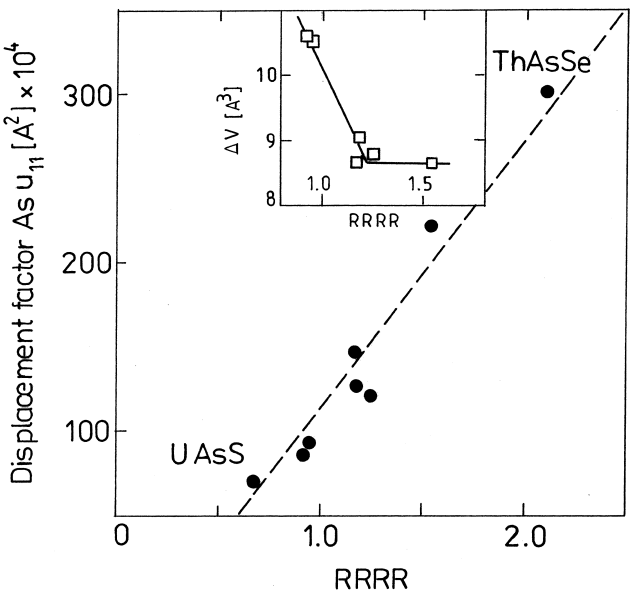

Fig. 6. Difference between the unit cell volume of ThAsSe and UAsSe (ΔV) and the anisotropic displacement factor for the arsenic ion (As u_{11}) as a function of reciprocal residual resistivity ratio (RRRR = $\rho(4,2)/\rho(300)$). The highest and lowest black circles represent ThAsSe and UAsS, respectively, while the remaining black circles and squares represent UAsSe.

from different phenomena. But for any further discussion on this problem it would be worthwhile to await an explanation of the role played by the shift of the 3.5% of the uranium ions from its proper position in the lattice. Furthermore, it is known that the discrepancy factor R is higher for the higher absorption coefficient. To reduce the latter, the examined specimens were shaped to a sphere or a cube of dimension smaller than about 0.4 mm while the specimens of irregular shape were smaller than 0.15 mm. Thus, we could reach $2 < R < 6$ (Table 1). On the other hand, the crystal data displayed in Tables 1 and 2, show no clear correlation between R and displacement factor. For instance, the As u_{11} is bigger for higher R value in the case of specimens UAsSe 108-1 and UAsSe 108-3 while this relation is reversed in the case of the UAsSe 116-1 and UAsSe 116-2 specimens. Also, both the lowest R ($=2.22$) specimen — UAsS — and the highest R ($=5.97$) specimen — ThAsSe — show the enhanced As u_{11} values over the general correlation shown in Fig. 6. Therefore, we think that if there is any correlation between the absorption coefficient and the displacement factor, the correlation between the latter and the RRRR seems to be much stronger. Thus, a simple interdependence between the As u_{11} and RRRR factors may mean either that the anisotropic displacement factor controls the RRRR one or both of them have the same origin.

6. Summary and discussion

As we documented above, the possible explanation of the origin of the nonmagnetic Kondo-like resistivity behaviour for the uranium and thorium arsenoselenides can be given in terms of the TLS Kondo model. The simplest realisation of the TLS is that of an atom which may sit in double well potential. The two wells being localised along a line directed between their centres, which are separated by the displacement vector. In the case of the TLS Kondo effect one should think of the position of the atom in one well or the other as an Ising spin variable. Electrons may 'flip' the spin by assisting the tunnelling between the wells [10]. Thus, such a nonmagnetic TLS centre has an internal degree of freedom, which is necessary for the Kondo effect. Hence, it may be responsible for the observed Kondo-type scattering of conduction electrons in the materials we studied.

The original motivation for studying such a model was the observation of logarithmic anomalies in the resistivity of metallic glasses [11–13]. There, the positional disorder of the atoms could just lead to the TLS of individual atoms. For example, $Pb_{1-x}Ge_xTe$ is the only crystalline compound that we know which exhibits logarithmic temperature dependence of the resistivity over one decade of temperatures [32], and it was shown to fit to the TLS Kondo model [33]. PbTe is a semiconductor, but when a small amount of Pb is replaced by Ge it transforms to a degenerate semiconductor. Because the ionic radius of Ge^{2+} of 0.73 Å is much smaller than the 1.2 Å radius of Pb^{2+}, the Ge atoms slide around, giving rise to a TLS. Though, the exact source of TLS in this material is known, however, the ambiguity arises because of the fact that the charge carrier concentration cannot be controlled in a systematic way [10].

The interdependence between the displacement factors and RRRR permits us to ascribe both the phenomena to the same origin. It suggests that the two-level system Kondo model is a suitable one for the theoretical description of the systems examined by us. Since, the displacement factor for all the atoms composing a given compound depends on RRRR (roughly in a similar way to that shown in Fig. 6 for As u_{11}) hence, we are not able to point out the exact source of the TLS. Moreover, the electron microscopy investigations of ThAsSe presented here and for UAsSe ($T_C = 108$ K) studied previously [8], have shown the perfect ordering of the cation sublattice. On the other hand, the neutron diffraction studies have indicated disorder in the anion sublattice UAsSe [8], which presumably depends on the As/Se ACR. It seems that rather a group of atoms than one single occupied lattice site is responsible for the TLS of the uranium and thorium arsenoselenides.

Though, an exact source of TLS in the uranium and thorium arsenoselenides is not known, we think that these systems have several advantages as compared to that of the $Pb_{1-x}Ge_xTe$ one: (i) the samples with desired TLS Kondo property of uranium and thorium arsenoselenides is easier to get than in the case of the latter compound, (ii) it is possible to study the TLS Kondo behaviour in nonmagnetic ThAsSe and in ferromagnetic UAsSe systems as well as in their solid solutions, (iii) a possible variation of the carrier concentration may rather tune the examined properties than make a dramatic change. For example in the case of the examined uranium arsenoselenide crystals, the possible variation of the As/Se atomic content ratio determines the change in the valence electrons by 0.12 per formula unit. (iv) It is possible to extend the family of TLS Kondo compounds studied here by other similar materials. As an example we can mention the UPS which is a ferromagnet below 118 K and shows the logarithmic anomalies in the resistivity [34]. Ref. [35] presents more representatives of the PbFCl family of actinide compounds.

We conclude with the observation that without doubt the existence of the correlation between the Kondo resistivity and the anisotropic thermal displacement factor of ions in the uranium and thorium arsenoselenides permits us to ascribe these systems to the TLS Kondo materials. The observed anomalously large displacement factors in the materials discussed above reflect also the possibility that the TLS formation is induced by the anion disorder. Thus, the PbFCl family of actinide compounds allows one to study a pure effect of the partial disorder in crystalline

nonmagnetic or ferromagnetic systems, on a Kondo-type behaviour as we have indicated in the above discussion.

Acknowledgements

This work was supported by the Polish Committee for Scientific Research, grant no. KBN-2 P03B 062 18; 2000–2001.

References

[1] Z. Henkie, R. Fabrowski, A. Wojakowski, Acta Phys. Polon. A 85 (1994) 249.
[2] Z. Henkie, R. Fabrowski, A. Wojakowski, J. Alloys Comp. 219 (1995) 248.
[3] K.P. Belov, A.S. Dmitrievsky, A. Zygmunt, R.Z. Levitin, W. Trzebiatowski, Zh. Eksp. Teor. Fiz. 64 (1973) 582.
[4] J. Leciejewicz, A. Zygmunt, Phys. Stat. Sol. A13 (1972) 658.
[5] A. Zygmunt, M. Duczmal, Phys. Stat. Sol. A 9 (1972) 659.
[6] A.C. Hewson, in: The Kondo Problem to Heavy Fermions, Cambridge Press, Cambridge UK, 1993.
[7] Z. Henkie, T. Cichorek, R. Fabrowski, A. Wojakowski, B.S. Kuzhel, Cz. Marucha, M.S. Szczepaniak, J. Tadla, Physica B 281–282 (2000) 226.
[8] Z. Henkie, T. Cichorek, A. Pietraszko, R. Fabrowski, A. Wojakowski, B.S. Kuzhel, L. Kępiński, L. Krajczyk, A. Gukasov, P. Wisniewski, J. Phys. Chem. Solids 59 (1998) 385.
[9] M.B. Maple, R.P. Dickey, J. Herrmann, M.C. de Andrade, E.J. Freeman, D.A. Gajewski, R. Chau, J. Phys.: Condens. Matter 8 (1996) 9773.
[10] D.L. Cox, A. Zawadowski, Adv. Phys. 47 (1998) 599.
[11] K. Vladár, A. Zawadowski, Phys. Rev. B 28 (1983) 1564.
[12] K. Vladár, A. Zawadowski, Phys. Rev. B 28 (1983) 1582.
[13] K. Vladár, A. Zawadowski, Phys. Rev. B 28 (1983) 1596.
[14] F. Hulliger, J. Less-Common Metals 16 (1968) 113.
[15] P. Wisniewski, A. Gukasov, Z. Henkie, A. Wojakowski, J. Phys-Condens. Matter 11 (1999) 6311.
[16] A. Wojakowski, Z. Henkie, Z. Kletowski, Phys. Stat. Sol. A14 (1972) 517.
[17] J. Schoenes, W. Bacsa, F. Hulliger, Solid State Commun. 68 (1988) 287.
[18] Z. Henkie, R. Fabrowski, A. Wojakowski, A.J. Zaleski, J. Magn. Magn. Mater. 140–144 (1995) 1433.
[19] P.M. Oppeneer, M.S.S. Brooks, V.N. Antonov, T. Kraft, H. Eschrig, Phys. Rev. B53 (1996) 1.
[20] W. Reim, J. Schoenes, F. Hulliger, Physica B 130 (1985) 64.
[21] W. Reim, J. Magn. Magn. Mater. 58 (1986) 1.
[22] A. Wojakowski, Z. Henkie, Acta Phys. Polon. A 52 (1977) 401.
[23] A.J. Arko, J.J. Joyce, J. Sarrao, J.D. Thompson, L. Morales, Z. Fisk, A. Wojakowski, T. Cichorek, J. Supercond. 12 (1999) 175.
[24] J. Brunner, M. Erbudak, F. Hulliger, Solid State Commun. 38 (1981) 841.
[25] J.M. Fournier, E. Gratz, in: K.A. Gschneider Jr. et al. (Eds.), Lanthanides, Actinides, Physics-1, Handbook On the Physics and Chemistry of Rare Earths, Vol. 17, Elsevier, 1993.
[26] J. Kondo, Prog. Theor. Phys. 32 (1964) 37.
[27] S. Hovmöller, Ultramicroscopy 41 (1992) 121.
[28] R. Wawryk, private communication.
[29] J.M. Leger, K. Oki, A.M. Redon, I. Vedel, J.M. Rossat-Mignod, O. Vogt, Phys. Rev. B33 (1986) 7205.
[30] T. Cichorek, Z. Henkie, P. Gegenwart, A. Wojakowski, M. Lang, F. Steglich, in: Sudeten Workshop on Anomalous Phenomena in d- and f-Electron Systems, Duszniki Zdrój, 25–28 May, 1999.
[31] A. Blaise, R. Lagnier, A. Wojakowski, A. Zygmunt, M.J. Mortimer, J. Low Temp. Phys. 41 (1980) 61.
[32] S. Takano, Y. Kumashiro, K. Tsuji, J. Phys. Soc. Japan 53 (1984) 4309.
[33] S. Katayama, S. Maekawa, H. Fukuyama, J. Phys. Soc. Japan 56 (1987) 697.
[34] D. Kaczorowski, H. Noel, M. Potel, A. Zygmunt, J. Phys. Chem. Solids 55 (1994) 1363.
[35] P. Santini, R. Lemanski, P. Erdos, Adv. Phys. 48 (1999) 537.